ZnO nanorod arrays with tunable size and field emission properties on an ITO substrate achieved by an electrodeposition method*

Gong Jiang-Feng(巩江峰)[a)b)†], Dou Zhao-Ming(窦召明)[a)], Wang Zhi-Qiang(王志强)[b)], Zhang Bo(张 博)[a)b)], Zhu Wei-Hua(朱卫华)[a)], Zhang Kai-Xiao(张开骁)[a)], Liu Ming-Yi(刘明熠)[a)], Zhu Hao(朱 浩)[c)], and Zhou Jian-Feng(周剑锋)[c)]

[a)] *Department of Physics, Hohai University, Nanjing* 210098, *China*

[b)] *National Laboratory of Solid State Microstructures, Nanjing University, Nanjing* 210093, *China*

[c)] *College of Engineering and Applied Sciences, Nanjing University, Nanjing* 210093, *China*

(Received 20 November 2011; revised manuscript received 5 December 2011)

In the present work, vertically aligned ZnO nanorod arrays with tunable size are successfully synthesized on nonseeded ITO glass substrates by a simple electrodeposition method. The effect of growth conditions on the phase, morphology, and orientation of the products are studied in detail by X-ray diffraction (XRD), scanning electron microscopy (SEM), and transmission electron microscopy (TEM). It is observed that the as-prepared nanostructures exhibit a preferred orientation along *c* axis, and the size and density of the ZnO nanorod can be controlled by changing the concentration of $ZnCl_2$. Field emission properties of the as-synthesized samples with different diameters are also studied, and the results show that the nanorod arrays with a smaller diameter and appropriate rod density exhibit better emission properties. The ZnO nanorod arrays show a potential application in field emitters.

Keywords: ZnO nanorod, microstructure, electrodeposition, field emission properties

PACS: 81.07.Bc, 81.15.Pq, 79.70.+q **DOI:** 10.1088/1674-1056/21/6/068101

1. Introduction

The synthesis of nanostructured semiconductor materials has attracted much attention from both the fundamental point of view and the increasing number of potential practical applications. In particular, wide band gap II–VI semiconductor nanostructures have aroused a great interest as optoelectronic materials with functions in flat-panel displays, field-effect thin film transistors, light-emitting diodes, and single-electron transistors.[1−5] ZnO, a new type of semiconductor with a large bandgap in the UV range (3.37 eV) and a large exciton binding energy of 60 meV,[1] has attracted extraordinary attention in the past decade because of its high mechanical strength, chemical stability, ambient insensitivity, and thermal stability, which allow it to be used in many fields, such as solar cells,[6] gas sensors,[7] field emission devices,[8,9] light-emitting diodes,[10] and so on.

Up to now, ZnO nanostructures with various forms including nanobelts,[11] nanowires,[12] nanorods,[13,14] nanoneedles,[15] nanotubes,[16] and nanoplates[17] have been synthesized. Recently, Wang and Song[18] demonstrated that mechanical energy can be converted into electrical energy using ZnO nanorod arrays as an agent, which indicates that the ZnO nanorod arrays are the most important nanostructures in the ZnO family. To date, various methods have been developed to synthesize the ZnO nanorods, such as metal–organic chemical vapour deposition,[19] thermal evaporation,[20] pulsed laser deposition,[21] and chemical vapour transport.[22] Usually, these methods are operated in a vacuum and/or at high temperature, and thus often require expensive and sophisticated equipment. In particular, the use of gold as nucleation and growth seeds has been the most successful method for the nanowire synthesis process. However, the Au atom may substitute the Zn atom during the growth process, which will significantly affect its phys-

*Project supported by the National Natural Science Foundation of China (Grant No. 11004047), the China Postdoctoral Sustentation Fund (Grant No. 200904501062), Jiangsu Provincial Postdoctoral Sustentation Fund, China (Grant No. 0901001B), and the Fundamental Research Fund for Central Universities (Grant Nos. 2010B09514 and 2010B29014).

†Corresponding author. E-mail: jfgong@hhu.edu.cn

© 2012 Chinese Physical Society and IOP Publishing Ltd

ical properties. It is still a challenge to synthesize the ZnO nanorod array at low temperature with neither seed nor catalyst.

Electrochemical deposition technique is an attractive electrosynthetic alternative to the conventional deposition method because the electrochemical deposition is a simple and cheap technique operated at ambient temperature and pressure, and it is convenient to control the growth of the film. In addition, the method is appropriate for growing a large area of thin film and does not need to consider the shape of the substrate. In this paper, we successfully synthesize ZnO nanorod arrays with different morphologies on indium tin oxide (ITO) glass substrates via an electrochemical deposition method. The as-prepared products are characterized by scanning electron microscopy (SEM), transmission electron microscopy (TEM) and X-ray diffraction (XRD). Field emission properties of ZnO nanorod arrays with different morphologies are carefully studied to establish the relationship between them.

2. Experimental details

All chemicals were purchased from commercial sources, and were used without further purification. All solutions in this study were prepared with deionized water.

The electrodeposition was carried out in a three-electrode cell system, in which a piece of indium tin oxide (ITO) glass substrate was used as the working electrode, a saturated calomel electrode (SCE) served as the reference electrode and a zinc sheet was used as the counter electrode to ensure a constant Zn^{2+} concentration in the electrolyte. The ITO glass substrates were cleaned ultrasonically in detergent, deionized water and ethanol sequentially prior to the film deposition. The ITO substrate had a sheet resistance of 10 Ω/square, which was cut into strips with a width and length of 1.0 cm and 2.0 cm, respectively.

The electrodeposition parameters are described elsewhere.[23] In a typical procedure, the electrodeposition of ZnO was performed in a classic three-electrode electrochemical cell at a constant temperature of 70 °C by immersing the ITO substrate in an electrolyte bath. The electrolyte contained 0.1-M KCl (analytical grade, purity 99.5%) and various concentrations (5 mM, 1 mM, 0.5 mM, and 0.2 mM) of $ZnCl_2$ (analytical grade, purity 98%). An Electrochemical Workstation (Model CS350, Wuhan Corrtest Instrument Co. Ltd, China) was used to provide a constant potential of –1.0 V versus SCE. The growth process lasted 90 min. After the deposition, the substrate was removed from the electrolyte bath and immediately rinsed in flowing deionized water to get rid of the residual salt from the sample surface. By changing the concentration of $ZnCl_2$, we prepared four samples under different concentrations of $ZnCl_2$, named A (5 mM), B (1 mM), C (0.5 mM), and D (0.2 mM) respectively.

The morphologies of the product were investigated using SEM (Philips XL-30, FEI USA) and TEM (Tacnail-F20 operated at 200 kV, FEI, USA). For TEM observation, a drop of ethanol suspension containing ZnO nanorods which were scrapped from the substrate was deposited on a copper grid beforehand. The crystalline structure was detected by XRD (ARL XTRA, Themo Electron Co., USA) with Cu Kα radiation in a 2θ range between 20° and 60°, the working current and potential of the tube were 20 mA and 20 kV respectively. The field emission properties

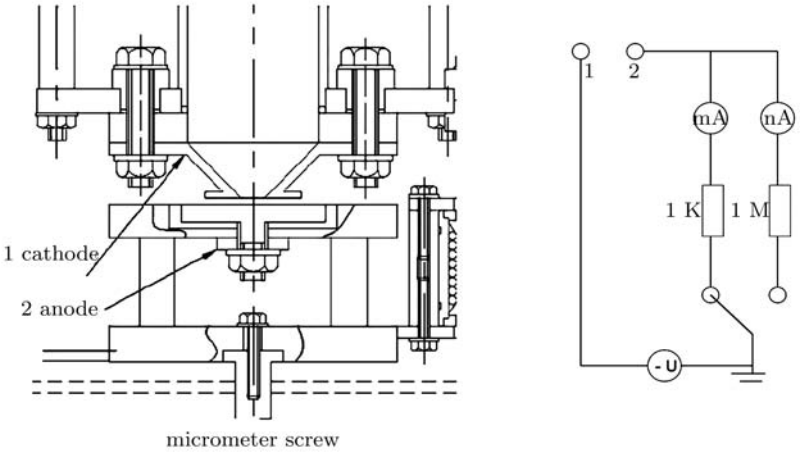


Fig. 1. Schematic diagram of the field emission measurement system.

were carried out under a pressure of 10^{-5} Pa in a lab-built field emission measurement system.[24] The as-synthesized sample was fixed on a stainless steel holder and used as a cathode, and a copper tip (frustum shape with 5-mm tip diameter) served as an anode. The distance between them could be adjusted by a micromanipulator outside the measurement chamber. The current data were acquired by changing the voltage applied between the cathode and anode in steps of 100 V.

3. Results and discussion

XRD is used to investigate the crystalline structure and phase purity of the as-synthesized ZnO product. The XRD patterns are shown in Fig. 2, which corresponds to samples A, B, C, and D respectively. As can be seen from the figure, except for the peaks of the ITO glass substrate (labeled by *), all the diffraction peaks can be well indexed to the hexagonal wurtzite structure of ZnO with lattice constants of $a = 0.325$ nm and $c = 0.521$ nm. The intensity of (0002) peak intensity at 34.4° became gradually stronger from sample A to sample D, which indicates that the orientation of the ZnO nanostructure can be well controlled by adjusting the electrolyte concentration. When the concentration of $ZnCl_2$ is 5 mM, the nanostructure (sample A) exhibits a c axis preferred orientation. Peaks from neither ZnO in other phases nor impurities are observed.

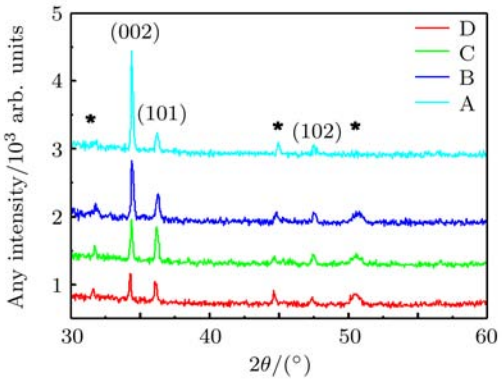


Fig. 2. (colour online) XRD patterns of the as-synthesized ZnO nanorod arrays.

In order to find the influence of the $ZnCl_2$ concentration on the morphology of the as-synthesized ZnO nanostructure, we study the morphologies of the samples synthesized under different $ZnCl_2$ concentrations systematically. The results are shown in Figs. 3(a)–3(d), which correspond to the SEM images of samples A–D respectively. It can be seen that the nanorods are nearly perpendicularly aligned to the substrate plane when the ZnCl2 concentration is 5 mM, and the nanorods are close to each other. The average diameter of the ZnO nanorods is 280 nm. As the concentration of ZnCl2 decreases from 2 mM to 0.2 mM, the average diameter of the nanorods becomes smaller gradually from 210 nm to 80 nm (the statistical nanorod diameters are shown in Table 1). Meanwhile, the density of the ZnO nanorods beomes smaller and smaller with the decrease in $ZnCl_2$ concentration and part of the nanorods lie on the substrate (see Fig. 3(d)). It should be noted that the size and density of the ZnO nanorod arrays can be easily controlled by adjusting the concentration of $ZnCl_2$.

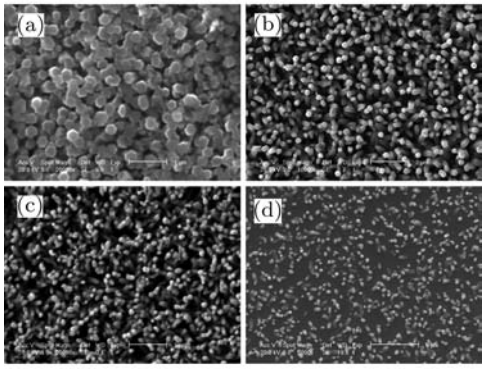


Fig. 3. SEM images of samples A (a), B (b), C (c), and D (d).

Table 1. Average diameter of ZnO nanorod arrays in the four samples respectively.

Sample	A	B	C	D
Diameter/nm	280	210	100	80

Further structural characterization of the ZnO nanorods is performed by TEM and high-resolution transmission electron microscopy (HRTEM). Figure 4(a) shows a typical TEM image of an individual ZnO nanorod which is taken from sample D. From the TEM image, it can be seen that the rod is straight and uniform with a diameter of about 80 nm, which is consistant with the results obtained from the SEM image (see Fig. 3(d)). The selected area of the electron diffraction (SAED) pattern (see the inset of Fig. 4(a)) indicates that the ZnO nanorod is a single crystal and of hexagonal wurtzite structure. Figure 4(b) displays a corresponding HRTEM image taken from the edge of the ZnO nanorod labeled in Fig. 4(a), which shows a perfect lattice structure. The lattice spacing is 0.520 nm and 0.281 nm, corresponding to the separation between two (0001) lattice planes and that

between two (2 –1 –10) lattice planes of hexagonal ZnO, respectively. The TEM results suggest that the nanorods grew along the *c* axis, which is in agreement with the XRD results. The energy dispersive X-ray spectroscopy (EDX) result (see Fig. 4(c)) shows that the nanorod is composed of O and Zn with an atomic ratio close to 1:1, confirming that the nanorod is ZnO. The C and Cu signals come from the supporting TEM carbon-coated copper grid.

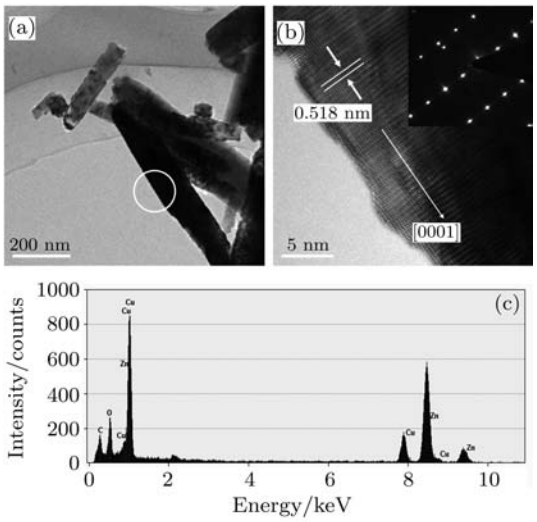


Fig. 4. (a) Typical TEM image of a ZnO nanorod; (b) HRTEM image of a ZnO nanorod, with the insert showing the corresponding ED pattern. (c) EDX image of a ZnO nanorod.

On the basis of the above experimental results, the growth process of ZnO nanorods is proposed as follows: in the electrodeposition process, the dissolved oxygen, serving as the oxygen source for the growth of ZnO, is reduced to OH^- ions near the cathode, following equation (1) and/or (2):[25,26]

$$O_2 + 2H_2O + 2e^- \rightarrow H_2O_2 + 2OH^-, \quad (1)$$

$$O_2 + 2H_2O + 4e^- \rightarrow 4OH^- \quad (2)$$

$$Zn^{2+} + 2OH^- \rightarrow ZnO + H_2O. \quad (3)$$

Follow Eq. (3), then $Zn^{2+}$and OH^- ions will react with each other, resulting in the formation of ZnO and its deposition on the substrate. As the potential is fixed at –1 V/SCE, the quantity of oxygen is high enough in the solution, and the concentration of OH^- ions is almost unchanged. Therefore the Zn^{2+} concentration will greatly affect the growth of ZnO. When the concentration of Zn^{2+} around the cathode is relatively high, it will produce more ZnO nuclei on the surface of the substrate at the beginning of the deposition process, leading to very high density of nuclei on the ITO substrate. Under these circumstances with enough Zn precursors, the reaction between Zn^{2+} and OH^- takes place not only at the top of the nanorods, but also surrounding the rods, which induces lateral and longitudinal growth simultaneously as shown in Fig. 5(a). On the contrary, when the Zn^{2+} concentration becomes lower, the number of OH^- ions is much more than that of Zn^{2+} ions at the surface of the substrate. This may reduce the production of ZnO nuclei because of the lack of zinc precursors, which will result in a lower density of nanorod arrays as shown in Fig. 4(d). On the other hand, although there are superabundant OH^- ions surrounding the ZnO nanorods, a low concentration of Zn^{2+} ions may lead to only enough Zn^{2+} ions existing at the top of the nanorods, facilitating the longitudinal growth of the nanorod. Meanwhile, lateral growth is suppressed due to the lower concentration of Zn^{2+} ions. Therefore, ZnO nanorods with relatively small diameters are obtained at a low concentration of Zn^{2+} ions as shown in Figs. 3(d) and 4(b).

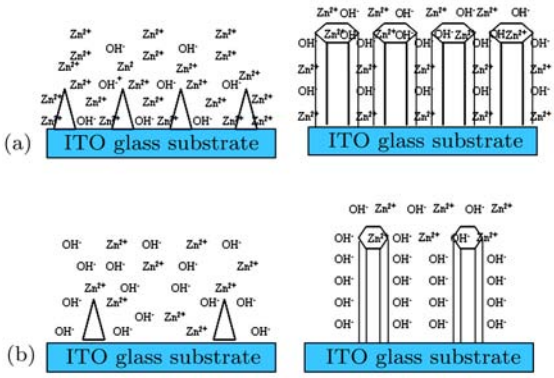


Fig. 5. (colour online) Schematic view of a possible growth mechanism of ZnO nanorods when: (a) the concentration of Zn^{2+} ions is high enough, (b) the concentration of OH^- ions is much higher than that of Zn^{2+} ions in solution.

Field emission properties of the as-synthesized ZnO nanorod arrays are studied in detail. A copper plate is used as an anode and a piece of ITO substrate with well-arranged ZnO nanorod arrays is used as a cathode. The distance between the electrodes is 100 μm. The turn-on field (E_{to}) and threshold field (E_{thr}) are defined as the electric fields that are required to produce current densities of 10 μA/cm^2 and 100 μA/cm^2 respectively. Figure 6(a) shows the dependences of the field emission current density (J) versus the applied electric field (E) of the ZnO nanorod

arrays synthesized under different Zn^{2+} concentrations. The E_{to} values of the samples A–D are 21.94, 15.76, 11.47, and 7.11 V/μm, respectively. Their E_{thr} values are 28.52, 22.62, 14.26, and 8.73 V/μm, respectively. The results are listed in Table 2. It is found that the ZnO nanorod array synthesized under a lower Zn^{2+} concentration exhibits the best field emission performance among the four samples.

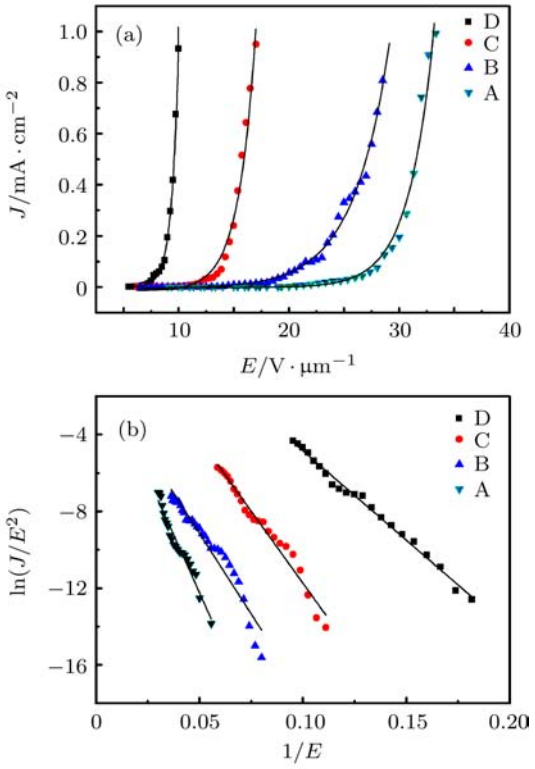


Fig. 6. (colour online) J–E curves for samples A, B, C, and D respectively and the corresponding Fowler–Nordheim (F–N) plots.

Table 2. Field emission properties of samples A, B, C, and D.

Sample	E_{to} /V·μm^{-1}	E_{thr} /V·μm^{-1}	β
A	21.94	28.52	328.9
B	15.76	22.62	410.9
C	11.47	14.26	535.6
D	7.11	8.73	896.3

To better understand the characteristics of emission current density Against an electric field of ZnO nanorod arrays, in this study we also analysed the current–voltage (I–V) data by using the Fowler–Nordheim (F–N) equation[27,28]

$$J = A\left(\frac{\beta^2 E^2}{\Phi}\right)\exp\left(-\frac{B\Phi^{3/2}}{\beta E}\right), \tag{4}$$

where J is the field emission current density, E is the applied field, Φ is the work function of the emitter and equal to 5.3 eV for ZnO,[29] A and B are approximate to two constants: 1.56×10^{-10} A·V^{-2}·eV and 6.83×10^3 V·eV$^{-3/2}\cdot$μm^{-1}, and β is the field enhancement factor. The above equation can be converted into other form as follows:

$$\ln\left(\frac{J}{E^2}\right) = -\frac{B\Phi^{3/2}}{\beta}\frac{1}{E} + \ln\left(\frac{A\beta^2}{\Phi}\right). \tag{5}$$

From Eq. (5), it can be seen that the factor of $-B\Phi^{3/2}/\beta$ is equal to the slope of the F–N plot (the curve of $\ln(J/E_2)$ versus $1/E$). The F–N plots of the as-synthesized ZnO nanorod arrays under different Zn^{2+} concentrations are shown in Fig. 6(b). All the curves are shown to be roughly linear at high applied fields, indicating that the emitting electrons result mainly from barrier tunneling electrons extracted by the electric field. Using the slope values of these curves and the data given above, the field enhancement factor β is calculated and shown in Table 2, from which we can see that the field emission from sample D follows F–N behaviour best with a higher β. On all occasions, the ZnO nanorods synthesized in the solution with 0.2-mM $ZnCl_2$ exhibit the best field emission properties with the lowest turn-on field, the lowest threshold field, and the highest field enhancement factor. We attribute these to several aspects shown below:

Field emission properties depend mainly on the morphology and density of the nanostructure.[30] In the field emission process, ZnO nanorods with a higher density can provide more emitters, but the screening effect between adjacent emitters will weaken their field emission capacity. The higher the nanorod density, the stronger the degree of the screening effect,[31] thus an appropriate density of the nanorods is needed to gain great field emission properties. On the other hand, ZnO nanorods with smaller diameters exhibit a lower turn-on field as well as a lower threshold field and a higher field enhancement factor.[31–34] In our experiment, benefiting from its small diameter and proper rod density, sample D achieves the greatest field emission properties.

4. Conclusion

ZnO nanorod arrays are synthesized on ITO glass substrates by a simple electrodeposition method under atmospheric conditions using neither a catalyst

nor a high temperature. The as-synthesized nanostructures each exhibit a c-axis preferred orientation with good crystallinity. By using different concentrations of $ZnCl_2$, ZnO nanorods with different diameters and rod densities are obtained. When the concentration of $ZnCl_2$ in electrolyte is lower, the diameter and the density will grow down correspondingly. A possible growth mechanism is proposed. Field emission properties of the as-synthesized samples are studied in detail. It is observed that the nanorod with a smaller diameter and appropriate rod density exhibits a better field emission performance with a lower turn-on field, lower threshold field, and higher field enhancement factor β, which we attribute to the screening effect between adjacent emitters. Further studies needs to be conducted.

References

[1] Chen Y, Bagnall D and Yao T 2000 *Mater. Sci. Eng.* B **75** 190

[2] Cui Y, Wei Q, Park H K and Lieber C M 2001 *Science* **293** 1289

[3] Negita K, Yamaguchi T and Tsuchie A 2003 *Appl. Phys. Lett.* **82** 2844

[4] Zayer N K, Greef R and Rogers K 1999 *Thin Solid Films* **352** 179

[5] Wang J, Gudiksen M S and Duan X 2001 *Science* **293** 1455

[6] Ismail B, Abaab M A and Rezig B 2001 *Thin Solid Films* **383** 92

[7] Vayssieres L, Keis K, Hagfeldt A and Lindquist S E 2001 *Chem. Mater.* **13** 4395

[8] Lee C J, Lee T J, Lu S C, Zhang Y, Ruh H and Lee H J 2002 *Appl. Phys. Lett.* **81** 3648

[9] Nakanishi Y, Miyake A, Kominami H, Aoki T, Hatanaka Y and Shimaoka G 1999 *Appl. Surf. Sci.* **142** 233

[10] Bao J M, Zimmler M A, Capasso F, Wang X and Ren Z F 2006 *Nano. Lett.* **6** 1719

[11] Lin C F, Lin H, Li J B and Li X 2008 *J. Alloy. Compd.* **462** 175

[12] Lee C J, Lee T J, Lyu S C, Zhang Y, Ruh H and Lee H J 2002 *Appl. Phys. Lett.* **81** 3648

[13] Sun Y, Fuge G M and Ashfold M N R 2004 *Chem. Phys. Lett.* **396** 21

[14] Gao X P, Zheng Z F, Zhu H Y, Pan G L, Wu F and Song D Y 2004 *Chem. Comm.* **12** 1428

[15] Li Y B, Bando Y and Golberg D 2004 *Appl. Phys. Lett.* **84** 3603

[16] Bonard J M, Mirko C, Ralph K, Olivier N and Nicolas W 2002 *Carbon* **40** 1715

[17] Pradhan D, Kumar M, Ando Y and Leung K T 2008 *J. Phys. Chem.* C **112** 7093

[18] Wang Z L and Song J H 2006 *Science* **312** 242

[19] Yi L X, Xu Z and Hou Y B 2001 *Chin. Sci. Bull.* **46** 1223

[20] Kong X H, Sun X M, Li X L and Li Y D 2003 *Mater. Chem. Phys.* **82** 997

[21] Zhang Y, Russo R E and Mao S S 2005 *Appl. Phys. Lett.* **87** 133115

[22] Huang M H, Mao S, Feick H, Yan H, Wu Y, Kind H, Web E and Yang P D 2001 *Science* **292** 1897

[23] Gong J F, Dou Z M, Ding Q P, Xu Y and Zhu W H 2010 *J. Nanomater.* **10** 7406289

[24] Song F Q, Zhang L, Han M, Huang H B, Li F, Ge J, Wan J G and Wang G H 2005 *J. Phys.* B: *Conden. Matter* **366** 200

[25] Strbac S and Adzic R R 1996 *Electrochem. Acta* **41** 2903

[26] Jiang S P, Cui C Q and Tseung A C C 1991 *J. Electrochem. Soc.* **138** 3599

[27] Frolov V D, Karabutov A V, Pimenov S M, Konov V I and Ageev V P 2001 *Diamond Relat. Mater.* **10** 1719

[28] Lee C J, Lee T J, Lyu S C, Zhang Y, Ruh H and Lee H J 2002 *Appl. Phys. Lett.* **81** 648

[29] Minami T, Miyata T and Yamamoto T 1998 *Surf. Coat. Technol.* **108** 583

[30] Cui J B, Daghlian C P, Gibson U J, Pusche R and Ley L 2005 *J. Appl. Phys.* **97** 044315

[31] Cao B Q, Teng X M, He S H, Li Y, Li G H and Cai W P 2007 *J. Phys. Chem.* C **111** 2470

[32] Jo S H, Lao J Y, Ren Z F, Farrer R A, Baldacchini T and Fourkas J T 2003 *Appl. Phys. Lett.* **83** 4821

[33] Wang Z Q, Gong J F, Su Y, Jiang Y W and Yang S G 2010 *Cryst. Grow. Des.* **10** 2455

[34] Huang J Z, Li S S and Feng X P 2010 *Acta Phys. Sin.* **59** 5839 (in Chinese)